PERGAMON

Electrochimica Acta 48 (2002) 153–163

ELECTROCHIMICA Acta

www.elsevier.com/locate/electacta

Non-isothermal ionic mass transfer at vertical parallel plate electrodes under natural convection. Comparison and validity range of dimensionless correlations

M.A. Pasquale [1], S.L. Marchiano [1], A.J. Arvia *,[1]

Instituto de Investigaciones Fisicoquímicas Teóricas y Aplicadas (INIFTA)-(Consejo Nacional de Investigaciones Científicas y Técnicas and Universidad Nacional de La Plata), Sucursal 4, Casilla de Correo 16, (1900) La Plata, Argentina

Received 14 August 2002

Abstract

For non-isothermal ionic mass transport-controlled electrochemical reactions on vertical parallel plate electrodes under steady state natural convection, the dimensionless correlation $Sh = 0.9\,(ScGr^*)^{1/4}$, Sh, Sc and Gr^* being Sherwood, Schmidt and Grashof number, respectively, earlier proposed (Electrochim. Acta 13 (1968) 1657; 14 (1969) 741), was extended covering almost two decades of $(ScGr^*)^{1/4}$. Data from different test reactions in the range $-10 \leq \Delta T' \leq 15$ °C, utilising cells of similar geometry and cathode height in the range $0.025 \leq X \leq 1$ cm were considered. Using the above correlation as reference, other dimensionless correlations later derived, considering data from the same test reactions and using electrochemical cells of approximately the same design, were critically reviewed. The validity range of these correlations covered a smaller range of $(ScGr^*)^{1/4}$ than the reference correlation, and their differences were explained in terms of cell designs and operating conditions.

Keywords: Mass transfer; Vertical electrodes; Non-isothermal convection; Silver electrodeposition

1. Introduction

Mass transport processes are often accompanied by heat transfer [1]. In natural convection these two processes have a definite and predictable influence on each other so they have been considered simultaneously. Non-isothermal natural convection affects the buoyancy force and the law of conservation of dissolved species. Buoyancy forces may approximately be represented as the sum of a contribution to the density change of the solution due to specific local changes in the solution concentration produced by reactions, and another one resulting from temperature gradients in the system. Earlier numerical solutions of basic equations for simultaneous heat and mass transfer under natural convection at a vertical plate have been obtained from the vaporisation of spray droplets to performance of packed catalytic reactors [2] and for laminar free convection at a vertical plate immersed in a liquid phase [3].

In electrochemical processes, particularly under free convection, non-isothermal situations arise from the Joule effect that may be either useful for self-heating, as occurs, for instance, in molten salt electrolysis, or deleterious in some electrochemical energy conversion devices [4–12]. In contrast to other variables that are programmed or measured in electrochemical reactions, such as potential, current, and hydrodynamic conditions, temperature as a driving force variable is seldom considered. In these cases, different either single or periodical temperature perturbation procedures and various cell designs have been utilised [13–22]. In any case, local temperature changes are relevant for both equilibrium and non-equilibrium properties of the system. It should be noted that the temperature dependence of electrode potentials and electrochemical reaction rates arise from different major contributions, such

* Corresponding author. Tel.: +54-221-425-7430/7291; fax: +54-221-425-4642

E-mail address: ajarvia@inifta.unlp.edu.ar (A.J. Arvia).

[1] ISE member.

0013-4686/02/$ - see front matter
PII: S0013-4686(02)00596-0

as the entropy changes reflected by the thermal coefficients of standard potentials, surface potential and concentration distribution associated with double layer effects, activation energy of charge transfer processes, and mass transport and conductivity [15].

The convective-diffusion equations for a vertical plate working electrode under stationary non-isothermal conditions were solved considering working electrode temperatures above and below the mean temperature of the solution [23–26]. The momentum, mass, and heat transfer equations were solved assuming that the streaming function is the algebraic sum of the streaming functions corresponding to concentration and temperature gradients. In this case, the Soret effect [27–29], as well as the influence of the advancing front on free convection that would appear for metal electrodeposition [30,31], were neglected. Then, the following expression for the average limiting current density ($\langle j_L \rangle$) was obtained [23],

$$\langle j_L \rangle = 0.90 D_i \, c_0 \left(\frac{\alpha^{3/4}}{Sc^{1/4}} \pm \frac{\beta^{3/4}}{Pr^{1/4}} \right)^{1/3} Sc^{1/3} \left(\frac{g}{4\nu^2} \right)^{1/4} X^{-1/4} \quad (1)$$

α and β being the densification coefficients

$$\alpha = \frac{c_0}{\rho_0} \frac{\partial \rho}{\partial c} \quad (2)$$

$$\beta = \frac{\Delta T'}{\rho_0} \frac{\partial \rho}{\partial T} \quad (3)$$

ν being the cinematic viscosity of the solution, D_i and c_0 the diffusion coefficient and concentration of the reacting species (i) in the bulk of the solution, respectively, g the gravity constant, and X the height of the working electrode. The expressions of Schmidt and Prandlt numbers are $Sc = \nu/D_i$ and $Pr = \nu\rho_0 C_p/\kappa$, respectively, C_p being the specific heat capacity at constant pressure, ρ_0 and κ the density and thermal conductivity of the solution, respectively, $\Delta T' = T_0 - T_c$, T_0 the average temperature between the anode and the cathode, and T_c the temperature of the working electrode. Eq. (1) was expressed as the dimensionless correlation

$$Sh = (0.9)(ScGr^*)^{1/4} \quad (4)$$

with

$$Gr^* = \left[\alpha^{3/4} \pm \beta^{3/4} \left(\frac{Sc}{Pr} \right)^{1/4} \right]^{4/3} \left(\frac{g}{4\nu^2} \right) X^3 \quad (4a)$$

$$Sh = \frac{j_L X}{n F c_0 D_i} \quad (4b)$$

The validity of Eq. (4) was first determined using electrochemical data from copper electrodeposition on copper under convection-diffusion control using aqueous copper sulphate + sulphuric acid solutions for both positive and negative temperature differences between the cathode and the anode (ΔT) [24]. The theory predicts that for a certain critical temperature gradient, convective effects resulting from the density gradients at the reaction interface due to local concentration changes and temperature gradients are counterbalanced. Experiments showed that around this critical temperature no steady cathodic current could be obtained as a result of the above-mentioned compensation effect. More recently, the validity of Eq. (4) has been proved by classical impedance and thermo-electrochemical transfer functions [32].

Simultaneously with the appearance of Eq. (4), the correlation

$$Sh = (0.63 \pm 0.05)(ScGr^*)^{0.243 \pm 0.07} \quad (5)$$

has been reported [33]. This correlation was also obtained from the analysis of copper electrodeposition data using a vertical plate electrode and a cell design in which the temperature on the working electrode surface was different from that at the inert part of the vertical wall, both lying on the same plane. This design introduces a relaxation length for the hydrodynamic boundary layer. As discussed further on, these facts can explain the somewhat distinct behaviour of correlations (4) and (5).

Another resolution of the non-isothermal convective diffusion differential equation for an electrochemical cell with parallel plate electrodes has been proposed [34,35]. In this case, the result has been obtained using the orthogonal collocation method, which led to the following dimensionless correlation,

$$\frac{Sh}{Gr_m^{1/4}} = 0.33 \, Sc^{1/4} \left\{ \left[1 + \left(\frac{Gr_t}{Gr_m} \right) Sc^{0.37} Pr^{-0.03} \right] + \left[1 + \left(\frac{Gr_t}{Gr_m} \right)^{3/4} Sc^{0.28} Pr^{-0.22} \right]^{1/3} \right\} \quad (6)$$

Gr_m and Gr_t being the Grashof numbers related to density changes produced by concentration changes from the electrochemical reaction and by the temperature gradient in the cell, respectively.

$$Gr_m = \frac{g\alpha X^3}{\nu^2} \quad (7)$$

$$Gr_t = \frac{g\beta X^3}{\nu^2} \quad (8)$$

In Eq. (6), the term in braces can be considered as a correction factor, $\Gamma(Sc, Gr, Pr)$, that depends on the three dimensionless numbers. Then, the form of Eq. (6) reduces to

$$Sh = 0.33(Sc \; Gr)^{1/4} \Gamma(Sc, \; Gr, \; Pr) \quad (8a)$$

Eq. (6) has been tested using electrochemical data

from the aqueous potassium ferro/ferricyanide redox reaction in the presence of an excess of potassium hydroxide. A concentric cylindrical cell design consisting of the inner wall of the outer cylinder as the working electrode and the outer wall of the inner cylinder as the counter electrode, has been utilised. The agreement between theory and experimental data has been estimated as 2% [35].

More recently, the influence of heating on the mass transport limiting current has also been considered for stationary disc electrodes of different diameters. As in previous cases, under non-isothermal conditions, mass transfer involves again a thermal convective contribution that is proportional to ΔT. The current ratio between non-isothermal and isothermal processes is given by

$$\frac{j_{\Delta T}}{j_{\Delta T=0}} = \left[1 + \left(\frac{Sc}{Pr}\right)^{1/4} \left(\frac{\beta \Delta T}{\alpha c_0}\right)^{3/4}\right]^{1/3} \quad (9)$$

Eq. (9) was tested using electrochemical data from the equimolar aqueous ferro/ferricyanide redox system in an excess of potassium chloride [36]. It holds true for electrodes of relatively large size and, according to the authors, when the radius of the electrode is decreased diffusion turns into three-dimensional hemispherical diffusion, i.e. for sufficiently small radii, the situation of a microelectrode is approached [37]. Accordingly, a steady diffusion current is observed in the absence of natural convection.

Non-isothermal convection on a heated disc electrode has also been investigated utilising data for copper electrodeposition from aqueous copper sulphate+sulphuric acid solution [38] and the experimental results have been expressed by empirical correlations valid within two ranges of values for the product $Sc \cdot Gr$. On the other hand, a number of approximate solutions for non-isothermal mass transport of importance for technical electrochemical reactors of different both geometry and flow conditions have been reported [39]. However, these approaches are beyond the scope of our work and are not considered in this paper.

The main objective of this work is to extent the validity of correlation (4) over a range of electrode heights covering from tenths of a mm, as has been used in cells for the electrochemical growth of quasi-bidimensional metal patterns [40,41], to cm. The extended range of Eq. (4) offers the possibility of revisiting correlations earlier reported, and discussing their validity range considering the assumptions made for their derivation and the design of experiments for testing them. For these purposes, the operating conditions and various electrochemical systems, cell and electrode dimensions, including the influence of the distance between the leading edges for diffusion and hydrodynamic flow on the limiting current, are critically considered.

2. Experimental

To study the influence of the working electrode height on the ionic mass transfer rate, electrochemical cells consisting of a vertical parallel plate cathode and anode made from either a silver sheet (Goodfellow, England, 99.999% purity) or nickel (99.99%) were utilised. The main test reaction was the electrodeposition of silver on silver from aqueous 0.024 M silver sulphate+x M sulphuric acid ($0.5 \leq x \leq 2.0$) that was prepared from analytical reagent quality chemicals and Milli-Q* water. Occasionally, to get rid of a possible interference of the growing metal front in the case of silver electrodeposition, runs involving the ionic mass transfer controlled ferro/ferricyanide electrochemical redox reactions on nickel electrodes with the same cell design were made. In this case, aqueous 0.05 equimolar potassium ferro/ferricyanide in 2 M sodium hydroxide was employed as the electrolyte solution. In all cases, freshly prepared working solutions were stored under nitrogen saturation. Sulphuric acid in the former case and sodium hydroxide in the latter were utilised as supporting electrolytes.

One set of cells (Fig. 1a and b) consisted of two horizontal glass plates separated by $X = 0.025$ cm equal to the electrode height, and cathode and anode width $W_c = 1.5$ and $W_a = 2.5$ cm, respectively, separated by $L = 2.3$ cm. To avoid border effects at the cathode, a mask made of 0.025 cm thick Teflon foil was symmetrically placed on both sides of the cathode to ensure a homogeneous primary current distribution on the cathode at the initiation of each run. This mask limited the effective cathode area to 0.037 cm^2, in contrast to 0.062 cm^2 area of the anode. The cathode and the anode were heated independently using a set of six 100 Ω–0.25 W resistors in a parallel arrangement. Each set of resistors was allocated on the upper face of a copper block (2.5 cm wide × 2 cm high × 1 cm long) and fed from an adjustable constant current source. LM 35 National sensors were placed in contact with the electrodes through appropriate holes made in the copper blocks. The temperature at each electrode/solution interface was determined very close to the electrode surface utilising YSI thermistors (Fig. 1a). Signals from thermistors were read with a Keithley multimeter model 173. As a first approach, the working temperature of each electrode was approximated by adjusting the current of each set of resistors. Then, the fine temperature adjustment and monitoring were made sensing the system with the YSI thermistors. Electrochemical runs were initiated after a thermal steady state was reached.

Another set of rectangular cells (Fig. 1c and d) was made of Lucite® using silver metal foil electrodes of height $X = 0.15$, 0.30 and 1 cm. The dimensions of the cathode and anode were $W_c = W_a = 1.5$ cm and $L = 2.3$ cm. The isolated counterface of each electrode was one

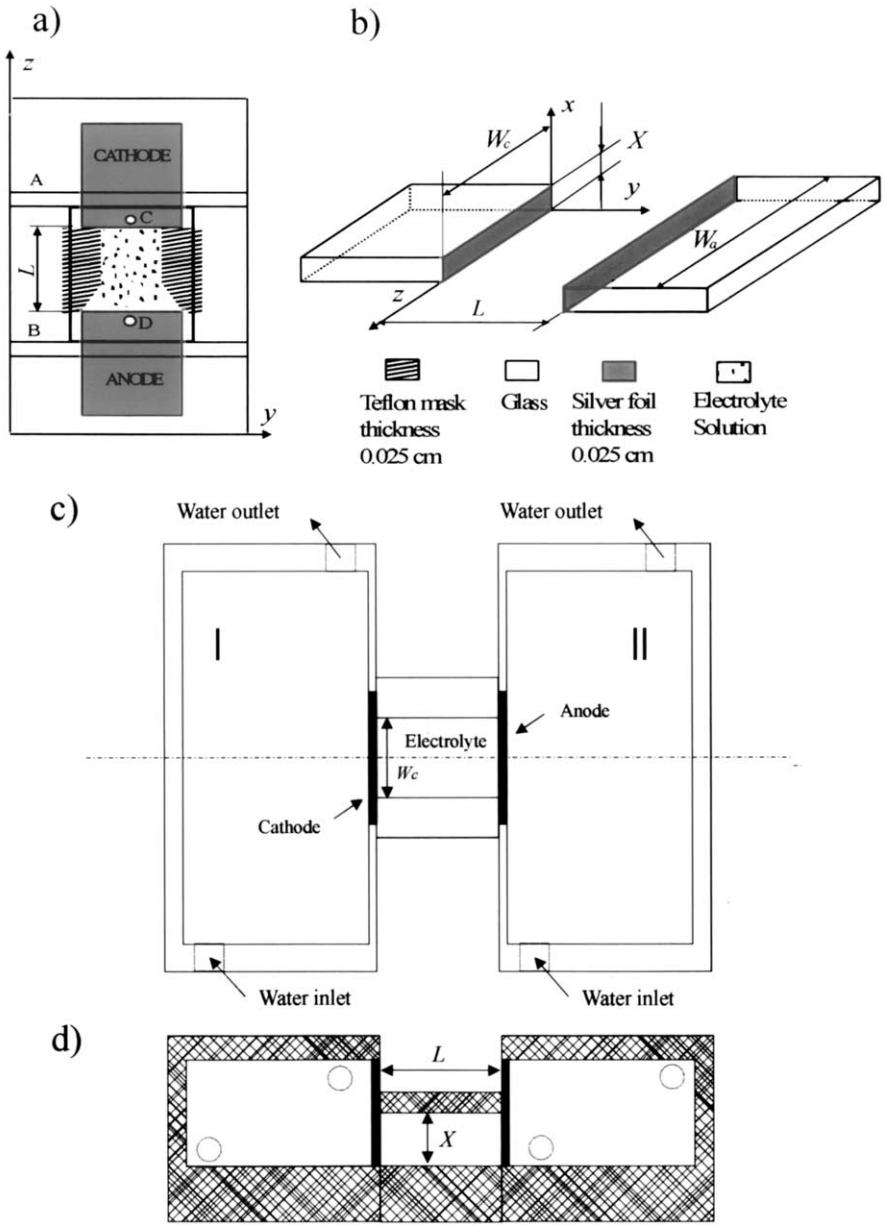

Fig. 1. Schemes of the electrochemical cells. (a) Top view of the cathode–anode arrangement at the quasi-bidimensional cell. Cartesian coordinates are indicated. (b) Perspective view of the electrodes and related geometrical parameters. (c) Top view of the the three-dimensional cell. (d) Cross section of the three-dimensional cell. I and II indicate the cathode and anode waterjacket for thermostatting.

wall of each rectangular box-shaped waterjacket (I and II). The temperature of the flowing water was controlled to ± 0.1 °C with a Lauda thermostat. Prior to each run, conventional cleaning procedures for the electrodes and the rest of the cell were used.

Both types of cell were operated in an 8 m^3 room thermally isolated from the laboratory environment. In this room the temperature fluctuation was ± 0.5 °C making the fine temperature control of the cell easier.

A Radiometer Voltalab potentiostat was utilised for electrochemical measurements. For runs made with the first set of cells, the cathode-to-anode potential was $\Delta E = -0.45$ V, and for the second one it was $\Delta E = -0.40$ V. As concluded from polarisation curves, both values of ΔE were in the range where the cathodic reaction was under ionic mass transfer control. The evolution of the cathodic current (I_c) and charge (Q_c) were followed over the entire range of electrodeposition time (t), although relevant data were obtained only in the range of time in which no appreciable influence of the electrodeposit roughness on the electrode area was noticed. For silver electrodeposition the anode, where silver electrodissolution proceeded, could be used as reference electrode. This was checked using as reference a silver wire electrode immersed in the working solution and placed in a separate compartment contacting the

solution in the cell through a capillary tip that was located at different distances from the cathode.

Experiments were made by adjusting the temperature of the cathode (T_c) in the range $15 \leq T_c \leq 40 \pm 0.05$ °C, and the anode temperature (T_a) was adjusted so that the values of $\Delta T'$ were in the range $-10 \leq \Delta T' \leq 20$ °C.

For the first type of cells, sequential photographs of growing silver electrodeposit profiles were taken using a stereoscopic microscope (Stemi 200 Zeiss) connected to a camera (Hitachi 220), coupled to a video screen and a computer equipped with a frame grabber and an image analyser (Contron Electronics KS300). From these images the evolution of the root mean square roughness (R_{rms}) of the growing front could be determined to establish the reliable ranges of t and Q_c for readings of I_L that could be referred to the initial geometric area of the working electrode with a minimum influence of roughness.

3. Results

3.1. Data from cells of variable height

3.1.1. Evaluation of the effective area of the cathode

Let us first estimate the range of time in which the influence of the electrode roughness on the cathodic limiting current remains lower than the experimental errors so that it can be disregarded. The electrodeposition of silver on polycrystalline silver is one of the fastest electrochemical reactions, as concluded from the corresponding exchange current density, $j_0 \cong 24 \pm 5$ A cm^{-2} [42,43]. Accordingly, under our operating conditions, the quasi-steady kinetics of this reaction is under ionic mass transfer control. However, due to the increase in the roughness of the deposit [44], the range of t in which I_L might be referred to the initial surface area of the cathode should be determined. For this evaluation we used data from both the cathodic current transients and the sequential imaging of the silver growing front.

For $X \geq 0.3$ cm, potentiostatic current transients (Fig. 2a) show that I_c decays in the range $0 \leq t \leq 20$ s, approaching a I_c versus $t^{-1/2}$ [45] relationship only for $t < 5$ s [46]. Subsequently, I_c reaches a minimum value, and later rises again up to a maximum value as natural convection sets in. The time at which the maximum current appears tends to be either lower or higher than for $\Delta T' = 0$, and it depends on whether $\Delta T'$ is negative or positive. This behaviour agrees with the dependence of I_L on $\Delta T'$ predicted by the theory of Eq. (4) that is referred to further on. Finally, a quasi-stationary cathodic current is attained. The same description also applies to data from experiments utilising cells with $X \cong 0.025$ cm, although in these cases, as seen from the I_c versus t plots (Fig. 2b), after the initial decay the current response becomes noisy. Thus, for the range $150 \leq t \leq 300$ s, I_c remains rather constant and for $t > 300$ s the increase in I_c is associated with a transition in the growth mode of the deposit and its increase in roughness [46].

The ratio Q_c/I_c versus t relationship expected from potentiostatic data (Fig. 3) depends on the mass transport contributions to the rate process and on whether the apparent cathode surface remains constant along the process. Thus, for pure diffusion, i.e. j_c depends linearly on $t^{-1/2}$, and the cathode surface is constant, the slope of the Q_c/I_c versus t plot is 2. On the other hand, for stationary free convection, i.e. j_c is constant, the slope of that plot is either 0.5 when the cathode area increases linearly with t or 1 when the apparent electrode surface is constant. The situation, however, becomes more complicated when the electrode area becomes a complex function of t. Experimental results for both ferricyanide ion electroreduction from equimolar 0.05 M aqueous potassium ferro/ferricyanide in 2 M sodium hydroxide for $X = 0.1$ cm, and silver electrodeposition for $X = 0.025$ cm (Fig. 3) show that pure diffusion is only approached for $t < 5$ s. For longer times, data from ferricyanide ion electroreduction behave rather close to the predictions of pure diffusion, whereas for silver electrodeposition, in the range $5 \leq t \leq 500$ s a slope closer to that predicted for steady free convective diffusion is observed. The difference in the behaviour of both reactions is consistent with the fact that the density change in the solution used for silver electrodeposition is much greater than that produced in the solution utilised for ferricyanide ion electro-reduction.

On the other hand, the sequential imaging of the silver growing front provides information about the evolution of roughness (R_{rms}). Values of R_{rms} were calculated from the equation [47]

$$R_{rms} = \left(\frac{1}{N}\right)\left\{\sum_i (h_{y,i} - \langle h_y \rangle)^2\right\}^{1/2} \quad (10)$$

$h_{y,i}$ and $\langle h_y \rangle$ being the maximum and average length of protrusion i (in the y-direction), respectively, N being the total number of protrusions, and $i = 1, 2, \ldots N$. Accordingly, the plot of R_{rms} versus t (Fig. 4) shows that the value of R_{rms} increases with t, but for the range $70 \leq t \leq 350$ s the value of R_{rms} remains approximately constant. Therefore, from the preceding results we can conclude that for $t < 350$ s, the influence of roughness on I_L becomes sufficiently small allowing us to express $j_L = I_L/A$ for both isothermal and non-isothermal runs, A being the initial area of the cathode.

3.1.2. Assessment of possible interferences

3.1.2.1. Cathode-to-anode distance. Another variable that should be critically considered is the minimum

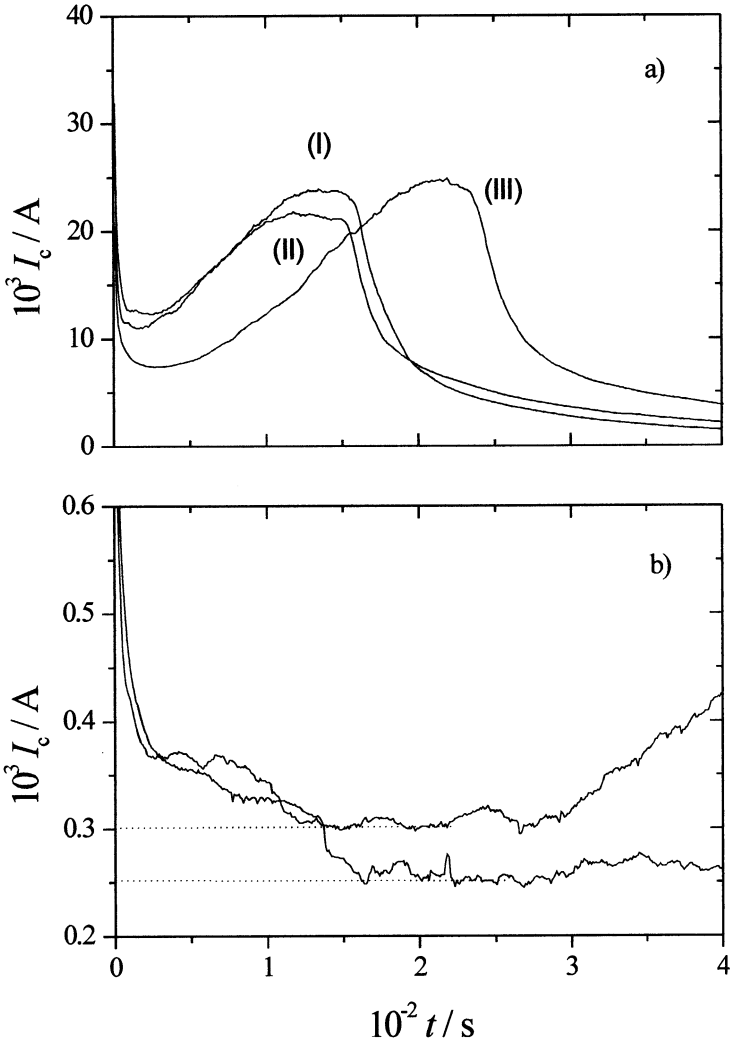

Fig. 2. (a) Potentiostatic current transients for silver electrodeposition from 0.024 M silver sulphate+0.5 M sulphuric acid run with the three-dimensional cell for $\Delta E = -0.40$ V; (I) $T_a = T_c = 27$; (II) $T_a = 22.5$ and $T_c = 27$; (III) $T_a = 35$ and $T_c = 27$ °C. The initial current approaches the I_c vs. $t^{-1/2}$ relationship. Current maxima are related to the contribution of free convection. For non-isothermal runs current maxima are either greater or smaller than that from the isothermal one depending on whether ΔT is negative or positive. (b) Potentiostatic current transients for silver electrodeposition from 0.024 M silver sulphate+0.5 M sulphuric acid run with the three-dimensional cell for $\Delta E = -0.45$ V. The initial current decay is comparable to that described in (a). The influence of free convection appears in the range $5 \leq t \leq 300$ s. For $t > 300$ s, the current increase is related to a transition in the growth mode and the increasing roughness of the electrodeposit [44].

cathode–anode distance (L) to assure that its value is at least twice the distance of the boundary layer at the cathode and anode in order to avoid their mutual interference. In this case, as the largest boundary layer thickness is related to heat transfer, the largest value of δ_T is estimated under the most unfavourable conditions using the dimensionless variable Λ [24].

$$\Lambda = \left(\frac{g\beta}{4\nu^2 X}\right)^{1/4} y \tag{11}$$

considering $y = \delta_T$ and $\Lambda = \Lambda_0$, i.e. when the value of the streaming function tends to zero [25].

For both types of cells the thermal and diffusion boundary layers start at the same point (Fig. 1), therefore, X is taken as the total height of the electrode. Data were calculated at different values of X taking $\Lambda_0 = 0.810$ and $\nu = 9.500 \times 10^{-3}$ cm^2 s^{-1} (Table 1). The dependence of δ_T on X is given by $\delta_T = 0.168\ X^{1/4}$. Consequently, the dimensions of both types of cells are adequate for our experiments.

3.1.2.2. The Stefan effect.

For both isothermal and non-isothermal conditions, the formation of a solid electro-deposit would imply that the advance of the growing front into the solution side brings forth a contribution to mass transfer processes. This complicated problem, known as the Stefan problem, might be relevant for our moving interface [29–31,48]. Accordingly, for a realistic appreciation of how large the magnitude of this effect could

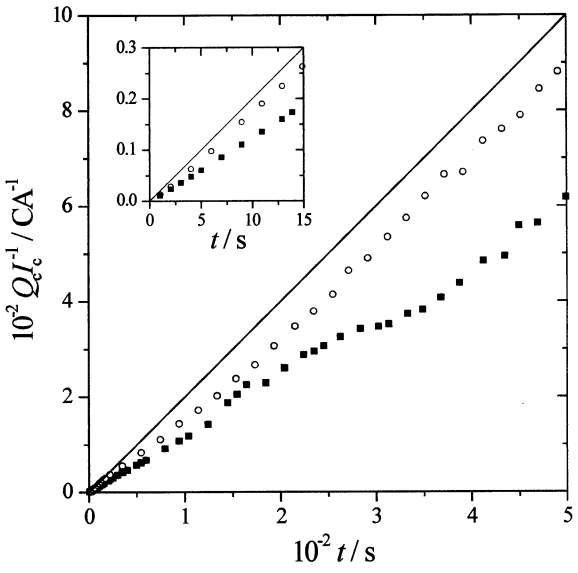

Fig. 3. Q_c/I_c vs. t plot from potentiostatic current transients resulting from different cathodic processes for $T_a = 30$ °C = T_c. (○) Data from aqueous equimolar 0.05 M potassium ferro/ferricyanide in 2 M sodium hydroxide, 25 °C. (■) Data from silver electrodeposition as indicated in Fig. 2a. The full trace corresponds to pure diffusion behaviour. The inset corresponds to the expanded initial region of the plot.

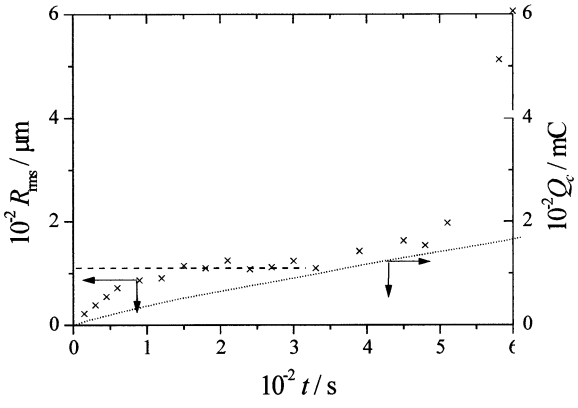

Fig. 4. R_{rms} and Q_c vs. t plot. Data obtained from sequential profiles of the silver growing front. The operating conditions for silver electrodeposition are the same indicated in Fig. 2b. The dashed line was drawn as a visual guide for the range of constant R_{rms}.

Table 1
Values of δ_T for different X

X (cm)	δ_T (cm)
0.010	0.053
0.025	0.067
0.150	0.104
0.300	0.124
0.500	0.141
1.00	0.168
5.00	0.251

$\Lambda = \Lambda_0 = 0.810$; $\nu = 9.500 \times 10^{-3}$ cm^2 s^{-1}; $\partial\rho/\partial T = 1.965 \times 10^{-4}$ g cm^{-3} °C^{-1} and $\Delta T = 1$ °C.

be, the displacement velocity in the y-direction of the front of silver electro-deposit at different values of x, and the displacement velocity of inert suspended particles in the solution during the electrochemical process were determined.

The local velocity of the growth front (v_{gf}) in the range $0 \le x \le X = 1$ cm was determined using the electrochemical cell with $X = 1$ cm, and the average fluid velocity (v_{flow}) in the x- and y-direction was evaluated from the displacement of suspended inert particles in the solution after $t > 50$ s [49]. From these data one obtains $v_{flow} = 140$ μm s^{-1}, a figure which is of the same order of magnitude as the maximum value $V_x = 200$ μm s^{-1} calculated from the Navier–Stokes equation [23,46], and $v_{gf} = 32$ μm s^{-1} for the local cathode $x \to 0$; $v_{gf} = 21$ μm s^{-1} for $x \cong 0.5$ cm and $v_{gf} = 7.2$ μm s^{-1} for $x \cong X = 1$ cm. Conversely, using the electrochemical cell with $X = 0.025$ cm, $v_{gf} = 8$ μm s^{-1}, and the maximum calculated value results in $V_x = 33$ μm s^{-1}. These figures are comparable to those that have been measured for a similar cell [50]. Likewise, data indicate that the influence of the advancing front on mass transfer depends inversely on the cathode height. On the other hand, for $X = 0.025$ cm the maximum influence of the advancing front velocity on free convection turns out to be about 24%. Then, the velocity of the moving front contributes to increase the value of Sh, particularly for small values of X, as will be described in Section 3.1.3.

Soret effect due to a temperature gradient is quite small [28], and therefore, it was disregarded.

3.1.3. Data processing according to Eq. (4)

For data processing the properties of the bulk of the solution at T_0 and at the cathode surface at T_c were considered. Thus, Sc was calculated at T_c, whereas Pr was evaluated at T_0. This procedure may not be strictly correct as far as the true average temperature and properties of solutions are concerned, but affords an appreciable simplification in the calculations, and introduces a minor error when compared to the assumptions made in the derivation of Eq. (4).

For the sake of calculating the $ScGr^*$ dimensionless group, the physicochemical properties of the solution were taken as concentration-independent. This situation is actually approached when the reacting ion is in the presence of an excess of supporting electrolyte. The density of the working solutions was determined picnometrically covering the range of temperature of our experiments and the range of electrolyte concentration resulting from the concentration changes produced by the electrochemical reaction at the cathode. According to Eqs. (2) and (3), the values of α and β were evaluated taking into account that $\partial\rho/\partial c_i = 1.886 \times 10^{-4}$ g mol^{-1}, and $\partial\rho/\partial T = 1.965 \times 10^{-4}$ g cm^{-3} °C^{-1}, respectively. Values of the diffusion coefficient of the

reacting ion D_i, the thermal conductivity κ, the specific heat capacity at constant pressure C_p, and the cinematic viscosity ν were taken from the literature [51]. These values together with the values of ρ, α, Pr and Sc for different T_0 are assembled in Table 2. Values of Sh calculated from the limiting cathodic current (I_L) under different experimental conditions are assembled in Table 3.

Results derived from both types of electrochemical cells and systems were plotted as $\log Sh$ versus $\log(ScGr^*)^{1/4}$ (Fig. 5). Data from the electrodeposition of copper on copper as test reaction, which have been obtained earlier [24] with a cell of a similar geometry and much larger size ($X=1$, $W=1$ and $L=4$ cm), were also included in this plot. The dotted line corresponds to Eq. (4). The agreement of experimental data and theoretical correlation is reasonably good and extends over almost two orders of magnitude for the product $(ScGr^*)^{1/4}$, i.e. covering the ranges $-10 \leq \Delta T' \leq +15$ °C and $0.025 \leq X \leq 1.0$ cm. The average error of all determinations referred to the theoretical slope is ± 0.01 and in the log–log plot the rms error is 0.07 and the probable error is ± 0.04.

Table 3
Values of the average limiting current and experimental Sh for different X, $\Delta T'$ and T_c; $W=1.4$ cm

T_c (°C)	$\Delta T'$ (°C)	X (cm)	10^4 I_L (A)	Sh
30.0	−6.8	0.025	2.7	3.0
30.0	−6.0	0.025	2.5	2.8
30.0	−2.5	0.025	2.7	3.0
30.0	0.0	0.025	3.1	3.4
30.0	2.5	0.025	2.1	2.3
30.0	5.1	0.025	2.2	2.4
30.0	7.5	0.025	2.9	3.2
30.0	8.2	0.025	3.2	3.6
30.0	9.4	0.025	3.0	3.4
30.0	11.6	0.025	2.7	3.0
30.0	15	0.025	3.4	3.7
35.0	0	0.025	2.7	2.7
35.0	−2.5	0.025	2.1	2.1
35.0	2.5	0.025	2.8	2.8
40.0	0.0	0.025	3.9	3.4
40.0	−2.5	0.025	3.4	3.0
30.0	3.3	0.15	10.8	5.6
30.0	6.5	0.15	18.5	9.6
30.0	8.5	0.15	15.0	7.8
30.0	0.0	0.30	28.9	15.0
30.0	6.5	0.30	35.8	18.5
30.0	8.5	0.30	34.8	18.0
45.5	9.3	1.00	95.0	52.6
47.0	8.5	1.00	73.0	37.8
43.0	6.5	1.00	73.0	37.8
45.5	7.8	1.00	93.5	48.4
45.0	2.5	1.00	97.5	40.1
40.0	0.0	1.00	96.5	39.7
40.0	−1.8	1.00	100.0	41.1
27.0	−2.3	1.00	97.0	53.7
0.0	−2.5	1.00	103.0	57.0
30.0	−4.0	1.00	120.0	62.2
40.0	−5.0	1.00	112.5	46.3

4. Discussion

4.1. General correlation applicable to available data

Experimental data confirms the validity of Eq. (4) for vertical plate electrodes using three different test reactions, two electrodeposition processes that are associated with the formation of relatively rough surfaces, and an electrochemical reaction in solution on a smooth electrode surface. The validity of Eq. (4) is extended over two orders of magnitude of the electrode height, and almost three orders of magnitude in terms of $(ScGr^*)^{1/4}$. It should be noted that for $\Delta T=0$ Eq. (4) becomes the isothermal correlation for ionic mass transfer under natural convection reported in the literature several decades ago [25,52,53].

On the other hand, limiting current density (j_L) data plotted in terms of j_L versus $\Delta T'$ (Fig. 6) show that $j_L \to 0$ when the value of $\Delta T'$ is around the critical value $(\Delta T')_{crit}$, i.e. the electrochemical system approaches non-steady diffusion. For silver electrodeposition $(\Delta T')_{crit} \cong 3.5$ °C. This behaviour, which is predicted by Eq. (1), involves exact opposing values of buoyancy

Table 2
Values of κ, C_p, ρ, ν, α, Pr and Sc at different T_0 foraqueous 0.024 M silver sulphate + 0.5 M sulphuric acid

T_0 (°C)	κ (J s cm^{-1} °C^{-1})	C_p (J g^{-1} °C^{-1})	ρ (g cm^{-3})	$10^2\nu$ (cm^2 s^{-1})	10^3 α	Pr	Sc
22.5	0.00578	4.1824	1.0207	0.9500	3.32	7.0	841
25	0.00582	4.1813	1.0202	0.8860	3.33	6.4	724
27.5	0.00586	4.1803	1.0198	0.8335	3.53	6.1	641
30	0.00590	4.1795	1.0192	0.7856	3.53	5.7	565
32.5	0.00594	4.1795	1.0187	0.7650	3.63	5.5	517
35	0.00598	4.1795	1.0183	0.7095	3.83	5.1	452
37.5	0.00602	4.1795	1.0178	0.6779	3.93	4.8	408
40	0.00606	4.1800	1.0173	0.6448	3.93	4.5	368
45	0.00614	4.1813	1.0163	0.5904	4.13	4.1	304
50	0.00622	4.1825	1.0153	0.5417	4.33	3.7	256

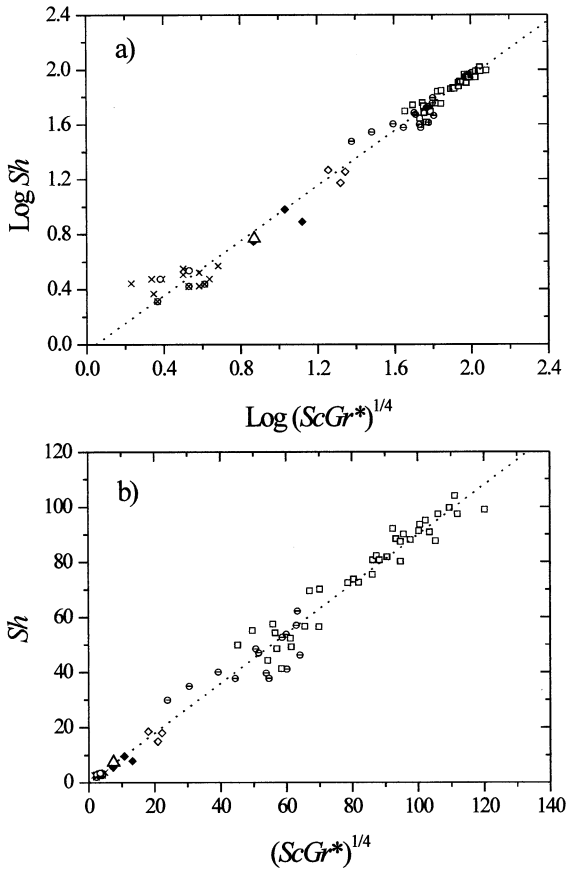

Fig. 5. Log Sh vs. $\log(ScGr^*)^{1/4}$ plot. Data from different electrochemical reactions, cell dimensions and temperature gradients. Silver electrodeposition from 0.024 M aqueous silver sulphate+0.5 M sulphuric acid: (×) $X=0.025$ cm, $\Delta E=-0.45$ V; (○) $X=0.025$ cm, $\Delta E=-0.475$ V; (◆) $X=0.15$ cm, $\Delta E=-0.40$ V; (◇) $X=0.3$ cm, $\Delta E=-0.40$ V; and (⊖) $X=1.0$ cm, $\Delta E=-0.40$ V. Silver electrodeposition on silver from 0.024 M aqueous silver sulphate+1.0 M sulphuric acid: (⊗) $X=0.025$ cm, $\Delta E=-0.45$ V. Ferri/ferrocyanide electroreduction on nickel using equimolar 0.05 M aqueous potassium ferro/ferricyanide in 2 M sodium hydroxide: (△) $X=0.10$ cm, $\Delta E=-0.40$ V; Copper electrodeposition on copper from 0.005 M aqueous copper sulphate+1.5 M sulphuric acid from Ref. [23]: (□) $X=1.0$ cm. The straight line corresponds to Eq. (4). The Sh vs. $(ScGr^*)^{1/4}$ plot (b) permits a clearer appreciation of data error.

forces that tend to produce the cancellation of free convection. Otherwise, for either $\Delta T' > (\Delta T')_{crit}$ or $\Delta T' < (\Delta T')_{crit}$ the system involves the opposite or co-operating buoyancy forces. Thus, for silver and copper electrodeposition processes under the conditions described above, co-operating buoyancy forces contribute to reinforce convection for $T_0 < T_c$, whereas the reverse situation appears for the ferricyanide ion electro-reduction undergoing in equimolar solutions containing an excess of supporting electrolyte.

For $t < 5$s only, i.e. in the range of time in which the development of free convection is still far from being completed, the advance of the growing front, due to the formation of a solid phase, modifies the rate of ionic mass transfer. This effect is also enhanced when $X \to 0$,

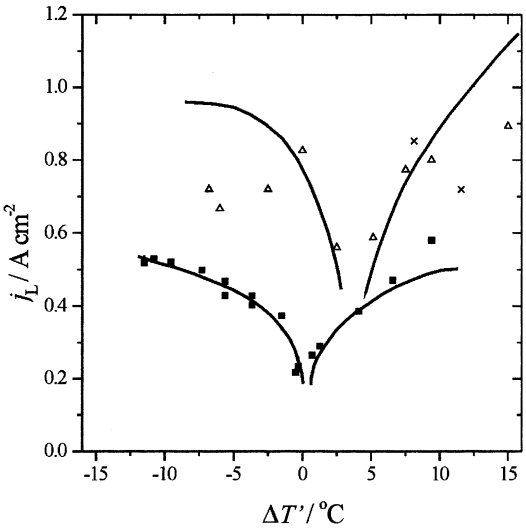

Fig. 6. Dependence of j_L on $\Delta T'$. Data from silver electrodeposition on silver using 0.024 M aqueous silver sulphate+0.5 (△) and 1.0 M (×) sulphuric acid. (■) Copper electrodeposition on copper from Ref. [24]. The solid traces correspond to the behaviour predicted by Eq. (1).

as can be concluded from data reported in Section 3.1.2.2.

4.2. Review of results from previous work

The processing of data obtained from a vertical plate electrode for the electrodeposition of copper on copper electrodes under simultaneous heat and mass transfer, plotted as $\log(Sh)$ versus $\log(ScGr_m)^{1/4}$, Gr_m being Grashof number related to isothermal free convection

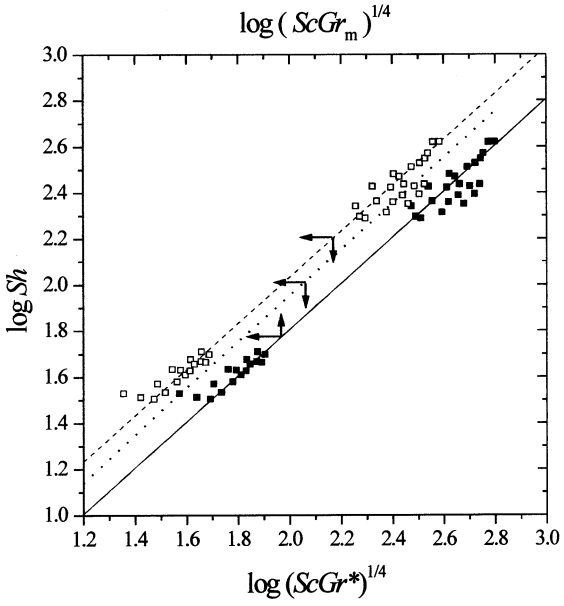

Fig. 7. Log Sh vs. $\log(ScGr_m)^{1/4}$ (■) and log Sh vs. $\log(ScGr^*)^{1/4}$ (□) plots. Non-isothermal data from Ref. [33]. Lower solid, middle dotted and upper dashed straight lines correspond to Eqs. (5) and (4), and Eq. (4) with data from Ref. [33], respectively.

(Fig. 7), fulfill Eq. (5) [33]. A critical analysis of the experimental set up used in there, indicates that additional effects appear to be involved in those experiments as compared to experiments performed utilising cells like those depicted in Fig. 1. The first effect is due to the fact that the vertical plate consisted of a copper plate electrode under temperature control and an inactive part at a different temperature that has been estimated empirically. Consequently, opposing buoyancy forces result at the upper and lower cathode border/inert plate edges. Unfortunately, for the cell design used in Ref. [33], the evaluation of these opposing buoyancy forces, which should contribute to the value of Gr^*, is unattainable. Nevertheless, from the effect of these buoyancy forces, one would expect lower Sh than those predicted by Eq. (4) for $ScGr^*$ constant. The second effect emerges from the uncertainty in the origin of the hydrodynamic and concentration boundary layers. One way to account for the influence of this effect would be by comparing data resulting from the definition of Gr_m as given in Ref. [33] to that of Gr^* from Eq. (4a). For this purpose it is convenient to reorder the expression of Gr_m in terms of α and β,

$$Gr_m = (gX/\nu)(\alpha + \beta(Sc/Pr)^2) \quad (12)$$

As shown in Fig. 7, for $ScGr$ constant, Eq. (5) (lower solid strait line) yields lower values of Sh than those resulting from Eq. (4) (dotted straight line). On the other hand, when our own data are recalculated using Eq. (12) taking $X = 1$ cm, $\Delta T = 15$ °C, $c_0 = 0.05$ M, $\nu = 0.0176$ cm^2 s^{-1}, $T_c = 5$ °C, $\alpha = 7.18 \times 10^{-3}$, $\beta = 6.49 \times 10^{-3}$, $Sc = 5590$ and $Pr = 9.1$, in all these cases, for constant Sh, the values of Gr_m are approximately eight times larger than those of Gr^*, i.e. the log–log plot resulting for Eq. (4) is shifted by approximately -0.23 unit in the x-direction from that corresponding to Eq. (5). Therefore, for constant $(ScGr)^{1/4}$, Gr being either Gr^* or Gr_m, values of Sherwood calculated from I_L measured in Ref. [33], turn out to be greater than those expected from Eq. (4) (upper dashed straight line), as one would expect from the existence of a relaxation length [25] that is actually included in the experimental device utilised in Ref. [33].

Another set of results [34,35] has been obtained with an electrochemical cell consisting of the gap between two concentrically arranged nickel cylindrical electrodes under temperature control each, using the potassium ferro/ferricyanide system as test reaction. The correlation of these data has been expressed by Eq. (7) derived for a vertical plate electrode in a semi-infinite space, covering laminar and turbulent regimes. Following the procedure referred to above, data from Ref. [34,35] were recalculated and plotted according to Eq. (4) as log Sh versus $\log(ScGr^*)^{1/4}$ (Fig. 8). This plot shows that for each series of experiments, the values of Sh for $\Delta T \to 0$ tend to remain constant, but for $\Delta T > |0.5$ °C|, data

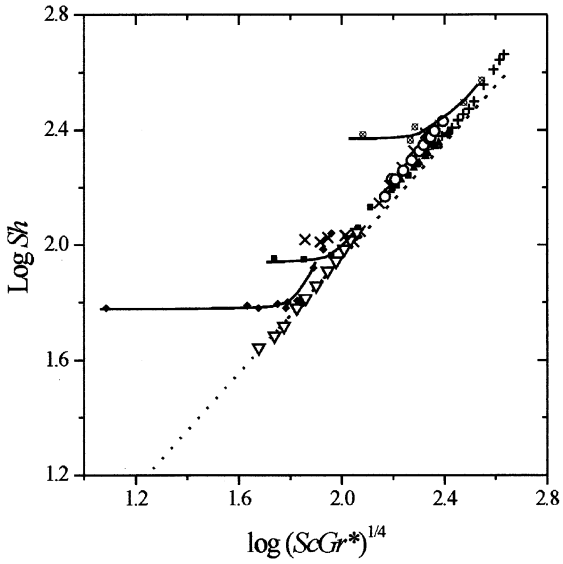

Fig. 8. Log Sh vs. $\log(ScGr^*)^{1/4}$ plot using non-isothermal data from Ref. [35] for the ferri/ferrocyanide electro reduction reaction on nickel from aqueous equimolar × M potassium ferro/ferricyanide in 0.5 M potassium hydroxide. (■) $x = 0.01$, $X = 5$ cm; (▽) $x = 0.01$, $X = 2$ cm; (×) $x = 0.03$, $X = 5$ cm; (◆) $x = 0.06$, $X = 2$ cm; (▲) $x = 0.06$, $X = 5$ cm; (○) $x = 0.06$, $X = 5$ cm; (⊗) $x = 0.06$, $X = 10$ cm; (+) $x = 0.06$, $X = 10$ cm. Dotted line corresponds to Eq. (4). Deviations occur when the temperature gradient is smaller than 0.5 °C.

approach the prediction of Eq. (4) very closely. Therefore, the largest portion of data involving a significant contribution of the thermal gradient to convection fulfils Eq. (4) reasonably well.

5. Conclusions

- The dimensionless correlation (Eq. (4)) for ionic mass transfer controlled electrochemical reactions on vertical plate electrodes under steady non-isothermal conditions was extended to cover temperatures above and below the mean temperature of the solution ($-10 \le \Delta T' \le 15$ °C), and cathode height in the range $0.025 \le X \le 1$ cm. This correlation has been derived by solving the momentum, mass and energy transfer equation assuming that the streaming function was the algebraic sum of the streaming functions for heat and mass transfer.
- The validity of the dimensionless correlation makes it possible to evaluate the free convection contribution for quasi-bidimensional rectangular electrochemical cells with parallel plate electrode arrangements with heights in the order of a tenth of mm. This is an interesting issue in dealing with the influence of mass transfer phenomena on the mechanism of solid pattern formation at the meso-scale.
- The extension of the dimensionless correlation (4) to more than two orders of magnitude in $\log(ScGr^*)^{1/4}$ renders the possibility of comparing it to other

correlations that have been proposed for the same type of processes at vertical plate electrodes and to envisage differences between the theoretical assumptions made in their derivation and the experimental approach to test them.

Acknowledgements

This work was financially supported by the Consejo Nacional de Investigaciones Científicas y Técnicas (CONICET) and PICT98 No. 06-03251 from Agencia Nacional de Promoción Científica y Tecnológica of Argentina.

References

[1] E. Somers, J. Appl. Mech. 23 (1956) 205.
[2] W.G. Mathers, A.J. Madden, E.L. Piret, Ind. Eng. Chem. 49 (1957) 961.
[3] W.R. Wilcox, Chem. Eng. Sci. 13 (1961) 113.
[4] D. Gidaspov, B.S. Baker, Am. Inst. Chem. Eng. J. 11 (1965) 825.
[5] H.F. Gibbard, J. Electrochem. Soc. 125 (1978) 353.
[6] P. Gallone, Trattato di Ingegneria Elettrochimica, Tamburini Editore, Milan, 1973, Chapter 16.
[7] K. Delimarkii, B.F. Markov, Electrochemistry of Fused Salts, Sigma Press, Washington, 1961, p. 90.
[8] K.W. Choi, N.P. Yao, J. Electrochem. Soc. 126 (1979) 1321.
[9] J.W. Lee, K.W. Choi, C.C. Christianson, J. Electrochem. Soc. 133 (1986) 1286.
[10] J.W. Lee, J.M. Hyun, Int. J. Heat Mass Transfer 34 (1991) 2409.
[11] Yu Chen, J.W. Evans, J. Electrochem. Soc. 140 (1993) 1883.
[12] F.H. Bark, F. Alavyoon, Appl. Sci. Res. 53 (1994) 11.
[13] J.S. Newman, W. Tiedemann, J. Electrochem. Soc. 142 (1995) 1054.
[14] F.H. Bark, Yu.I. Kharkats, R. Wedin, Russ. J. Electrochem. 34 (1998) 434.
[15] J.L. Valdes, B. Miller, J. Phys. Chem. 92 (1988) 525.
[16] G.C. Barker, A.W. Gardner, J. Electroanal. Chem. 65 (1975) 95.
[17] Y. Harima, S. Aoyagui, J. Electroanal. Chem. 69 (1976) 419.
[18] Y. Harima, S. Aoyagui, J. Electroanal. Chem. 81 (1977) 47.
[19] V.A. Benderskii, G.I. Velichko, J. Electroanal. Chem. 140 (1982) 1.
[20] C. Gabrielli, M. Keddam, J.F. Lizee, J. Electroanal. Chem. 148 (1983) 293.
[21] B. Miller, J. Electrochem. Soc. 130 (1983) 1639.
[22] J.F. Smalley, C.V. Krishnan, M. Goldman, S.W. Feldberg, Electrochem Soc. Meeting, Philadelphia, May, 1987.
[23] S.L. Marchiano, A.J. Arvia, Electrochim. Acta 13 (1968) 1657.
[24] S.L. Marchiano, A.J. Arvia, Electrochim. Acta 14 (1969) 741.
[25] B. Levich, Physicochemical Hydrodynamics, Prentice Hall, Englewood Cliffs, NJ, 1962, p. 127.
[26] A.P. Grigin, A.D. Davydov, Russ. J. Electrochem. 11 (1998) 1111.
[27] J.N. Agar, in: P. Delahay, C. Tobias (Eds.), Advances in Electrochemistry and Electrochemical Engineering, vol. 3 (Chapter 2), Interscience Publishers, John Wiley, New York, 1963, p. 81.
[28] J.S. Newman, Electrochemical System, 2nd ed., Prentice-Hall, Englewood Cliffs, NJ, 1991, p. 286.
[29] J. Cranck, Free and Moving Boundary Problems (Chpt. 1 and 2), Clarendon Press, Oxford, 1984.
[30] A.D. Solomon, in: D.G. Wilson, A.D. Solomon, P.T. Boggs (Eds.), Moving Boundary Problems, Academic Press, New York, 1978.
[31] S.R. De Groot, P. Mazur, Non-equilibrium Thermodynamics, North Holland, Amsterdam, 1962.
[32] I. Citti, O. Aaboubi, J.P. Chopart, E. Merienne, A. Olivier, Electrochim. Acta 41 (1996) 2731.
[33] J.A. De Leeuw den Bouter, B. De Munnik, P.M. Heerties, Chem. Eng. Sci. 23 (1968) 1185.
[34] P. Novak, I. Rousar, Collect. Czech. Chem. Commun. 44 (1979) 1857.
[35] P. Novak, I. Rousar, Collect. Czech. Chem. Commun. 48 (1983) 2213.
[36] Z.A. Rotenberg, A.V. Dribinskii, V.P. Lukovtsev, Russ. J. Electrochem. 35 (1999) 395.
[37] R.M. Whightman, D.O. Wipf, in: A.J. Bard (Ed.), Electroanalytical Chemistry, vol. 15, M. Dekker, New York, 1989.
[38] A.A. Wragg, A.K. Nasiruddin, Electrochim. Acta 18 (1973) 619.
[39] D.J. Tagg, M.A. Patrick, A.A. Wragg, Trans. I Chem E 57 (1979) 176.
[40] A.E. Bolzan, A.S.M.A. Hasseb, P.L. Schilardi, R.C.V. Piatti, R.C. Salvarezza, A.J. Arvia, J. Electroanal. Chem. 500 (2001) 533.
[41] A.S.M.A. Hasseb, A.E. Bolzan, P.L. Schilardi, R.C.V. Piatti, R.C. Salvarezza, A.J. Arvia, J. Electroanal. Chem. 500 (2001) 543.
[42] H. Gerischer, R.P. Tischer, Z. Elektrochem. 61 (1957) 1159.
[43] E. Budevski, W. Bostanov, T. Vitanov, Z. Stoinov, A. Kotzewa, R. Kaischev, Phys. Status Solidi 13 (1966) 577.
[44] M.A. Pasquale, P.L. Schilardi, S.L. Marchiano, R.C. Salvarezza, A.J. Arvia, Phys. Rev. E. 65 (2002) 041608-1.
[45] H.J.S. Sand, Philos. Mag. 1 (1901) 45
[46] M.A. Pasquale, S.L. Marchiano, A.J. Arvia, J. Electroanal. Chem., in press.
[47] A.-L. Barabási, H.E. Stanley, Fractal Concepts in Surface Growth, Cambridge University Press, Cambridge, 1995.
[48] A.A. Weeler, in: D.T.J. Hurle (Ed.), Handbook of Crystal Growth, vol. 1 (Chapter 10), Elsevier, Amsterdam, 1993, p. 693.
[49] M.A. Pasquale, S.L. Marchiano, A.J. Arvia, to be published.
[50] J.M. Huth, H.L. Swinney, W.D. McCormick, A. Kuhn, F. Argoul, Phys. Rev. E 15 (1995) 3444.
[51] International Critical Tables, vols. III and V, McGraw-Hill, New York, 1928.
[52] C.R. Wilke, M. Eisenberg, C.W. Tobias, J. Electrochem. Soc. 100 (1953) 513.
[53] C.R. Wilke, C.W. Tobias, M. Eisenberg, Chem. Engng. Progr. 49 (1953) 663.